J Geophys (1986) 59:98–102

Journal of Geophysics

Paleomagnetism of Miocene volcanism from South Syria

P. Roperch[1,2] **and N. Bonhommet**[2]

[1] ORSTOM département A, 213 rue Lafayette, F-75480 Paris Cedex 10, France
[2] Laboratoire de géophysique interne, Université de Rennes, Institut de Géologie, Campus de Beaulieu, Avenue de Géneral Leclerc, F-35042 Rennes Cedex, France

Abstract. Syrian Miocene alkali basalts have been sampled in the area south of Damascus. Thirty two flows were collected from short vertical sections (one to six flows) at ten sites. The sequence of polarity observed at each site is compatible with a magmatic event taking place during a reversal. Change of polarity and the presence of transitional directions allows: (1) correlation of flows between sites, (2) the assessment of the short duration of this volcanism. Moreover, the mean direction of magnetization ($D=179$, $I=-34$, $K=28$, $\alpha_{95}=6°$) shows clearly that since Miocene times no tectonic rotation occurred in this deformed area close to the east side of the Levant fault and south of the Palmyra chain.

Key words: Paleomagnetism – Arabia – Syria – Miocene – Basalt

Introduction

The opening of the Red Sea which started 20 My ago is responsible for a sinistral movement of 105 km along the Levant transform fault (Freund, 1965). In this area, large deformation occurs on both sides of the main fracture zone with the Lebanon mountain on the western part and the Palmyra Chain on the eastern part (Fig. 1). This tectonic setting has initiated early paleomagnetic studies which have been undertaken in Lebanon and Israel. The first results on Jurassic and Cretaceous formations from Lebanon showed large discrepancies with the apparent polar wander path of Africa and led to the concept of a Lebanese microplate (Van Dongen et al., 1967; Gregor et al., 1974). Further paleomagnetic work in Israel (Freund and Tarling, 1979; Ron et al., 1984) explains the results in terms of block rotation by strike-slip faulting. All these studies have been conducted on the western part of the Levant fault. Although there are fewer structural complexities on the east side of the Levant fault, no paleomagnetic results are available.

We have decided to sample the Miocene volcanic sequence, commonly related to the first stage of volcanic activity along the Levant fault, in Syria in order to provide a Miocene reference pole for this area or, on the contrary, to detect post-Miocene local deformation.

Offprint requests to: N. Bonhommet

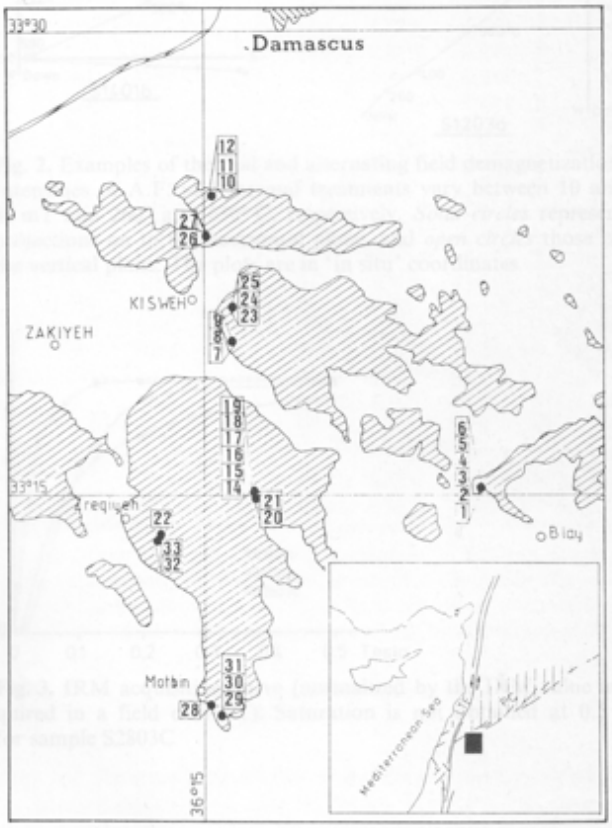

Fig. 1. Sampling map of the Miocene volcanism south of Damascus. For each site, the flow numbers are shown in their stratigraphic position. *The inset* shows the studied area in the major tectonic context. *LTF* Levant Transform Fault: *PC* Palmyra Chain

Sampling, laboratory techniques and measurements

The Miocene volcanism, composed of olivine alkaline basalt, outcrops in the Damascus region. The fact that this volcanism is involved in the Palmyra Chain constrains the age to the Miocene period. Thi interpretation is supported by radiometric Ar^{39}–Ar^{40} dating which gives an age of 19.5 Ma on one flow (No. 24). The volcanic sequence, which appears to be flat-lying, has been highly dissected by erosion. Fresh outcrops were found in quarries, from which all samples were taken. Because the lateral extent

of individual flows is not known, it is difficult to determine the total number of independent flows exposed in this sequence. The paleomagnetic sampling was done in small vertical sections of successive flows at different sites (Fig. 1). Thirty-two flows have been collected with a mean of four cores per flow oriented with both magnetic and sun compasses. The magnetic measurements were done with a computer-assisted Schonstedt spinner magnetometer. Thermal and A.F. demagnetization procedures were also carried out with Schonstedt equipment. The non-magnetic furnace and A.F. demagnetizing apparatus have a very low residual field of about 10 nT.

Results

Magnetic properties

The analysis of the NRM directions shows two types of behaviour. The first group corresponds to flows for which the demagnetization does not change the NRM direction. A very high stability of the remanence is found by alternating field as well as by thermal demagnetization. Some examples are shown on the orthogonal Zijderveld plots (Fig. 2). In some samples, a remarkable feature is the persistence of the NRM directions above the magnetite Curie point, indicating a remanent magnetization obtained by a high-temperature oxidation during the cooling of the flows (Fig. 2). This behaviour is seen on both normal and reversed samples. This is correlated with large median destructive fields and IRM acquisition curves for which saturation was not always obtained at 300 mT, a field high enough to saturate most magnetites (Fig. 3). Therefore, the contribution of hematite to the natural remanence is suggested. For the second group of flows, a random secondary component is generally removed by a low alternating field (20 mT). However, for higher fields, the magnetization direction becomes stable; an example is given in Fig. 2 by sample S0401b.

Table 1 shows the mean direction of magnetization for each flow obtained after stepwise A.F. or thermal cleaning and, for each sample, using the characteristic direction given from the orthogonal diagrams. Characteristic directions were isolated for 30 flows (Table 1).

We have not been able to determine the characteristic mean directions of flows S22 and S30; they were omitted from Table 1. The magnetization of samples from flow S30 consisted of both polarities as illustrated by stepwise thermal demagnetization of sample S3002 (Fig. 4). The orthogonal diagram reveals two anti-parallel directions: a normal component with blocking temperatures up to 490° C and a reverse component with higher blocking temperatures which can be followed above 560° C degrees. As this flow is intercalated between a reverse and a normal magnetized flow, we can interpret this result as a thermal overprint by the overlying flow which has a normal polarity. It is interesting to note that A.F. demagnetization was not successful in isolating the primary remanence component (Fig. 4). A reverse component is determined on two samples ($D=191$, $I=-23$) but, as an accurate determination of the primary component direction was not possible, the result for flow S30 was not included in Table 1. This result was only used for qualitative correlations between flows.

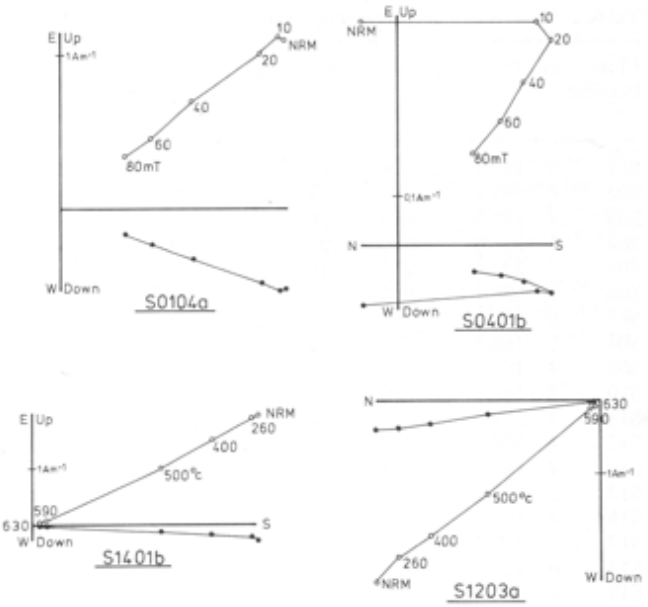

Fig. 2. Examples of thermal and alternating field demagnetization. Intensities of A.F. and thermal treatments vary between 10 and 80 mT and 260° and 630° C, respectively. *Solid circles* represent projections on to the horizontal plane, and *open circles* those on the vertical plane. The plots are in 'in situ' coordinates

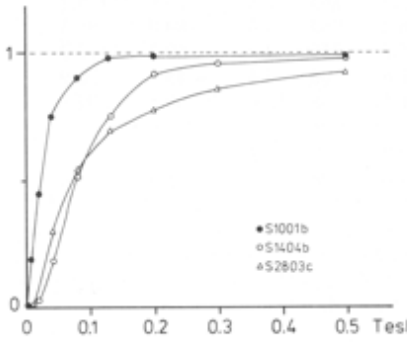

Fig. 3. IRM acquisition curve (normalized by the IRM value acquired in a field of 1.2 T). Saturation is not obtained at 0.5 T for sample S2803C

Paleomagnetic field record

Figure 5 shows the distribution of the mean directions of each flow. Normal and reverse polarities are present at three sites. Normal magnetized flows overlie those with reverse directions: moreover, at two other sites (S1–S6, S26–S27) intermediate directions overlie reversed directions. This magnetostratigraphy is consistent with the sampling of the same reversal of the earth's magnetic field at different sites of a volcanic sequence. In the section S14 to S19, a transitional direction (S18) is intercalated between two normal directions S17 and S19, suggesting that the normal polarity which has been recorded in flow S17 was not completely stable. It is interesting to notice that a similar behaviour (the field reversal occurs in two phases, the first attempt at reversal being unsuccessful) has been recorded in the Steens Mountain transition zone (Prevot et al., 1985) and in a lava sequence from Kauai (Bogue and Coe, 1982).

Table 1. Flow-mean paleomagnetic results

Flow number	N	D	I	K	α_{95}	VGP	
						Latitude	Longitude
S01	5	192.1	−41.0	182	5.7	−75.6	345.5
S02	4	191.9	−43.1	579	3.8	−76.8	341.2
S03	4	188.6	−45.5	561	3.9	−80.3	343.9
S04	5	201.4	−44.5	105	7.5	−70.2	321.3
S05	5	232.4	−30.6	21	17.1	−40.2	312.4
S06	5	233.7	−40.5	176	5.8	−42.1	303.8
S07	6	170.5	−39.8	143	6.0	−76.5	77.0
S08	5	168.3	−43.0	50	11.0	−76.9	90.4
S09	4	165.7	−34.9	88	9.9	−71.1	82.2
S10	5	169.6	−37.9	139	6.5	−74.9	76.5
S11	4	158.6	−42.1	73	10.8	−69.3	106.3
S12	4	354.5	42.6	126	8.2	80.2	241.1
S14	4	182.6	−22.8	922	3.0	−68.5	29.2
S15	5	183.3	−17.1	934	2.5	−65.4	28.4
S16	4	192.9	−34.9	263	5.7	−71.9	353.5
S17	5	359.2	18.6	250	4.8	66.3	218.2
S18	6	117.5	−14.8	435	3.2	−27.0	117.1
S19	4	17.8	15.6	601	3.8	59.9	179.1
S20	4	162.7	−43.3	150	7.0	−73.0	102.8
S21	4	183.7	−24.4	191	6.7	−69.5	25.6
S23	5	157.4	− 8.4	301	4.4	−54.2	77.1
S24	6	165.4	−40.6	236	4.4	−73.7	92.0
S25	6	182.8	−21.0	196	4.8	−67.5	29.0
S26	6	186.1	−38.4	216	4.6	−77.2	9.7
S27	3	305.2	45.2	109	12.0	42.6	313.6
S28	5	121.4	−13.7	863	2.6	−29.9	114.1
S29	4	170.4	−46.2	963	3.0	−80.0	94.3
S31	5	6.1	25.2	265	4.7	69.3	199.2
S32	5	179.5	21.8	108	7.4	−45.5	36.9
S33	5	7.7	−11.1	38	12.6	50.5	204.1
Mean	30	177.0	−32.2	9	9.3		
(1)	23	179.0	−34.0	28	5.9	−75.0	40.0

N is the number of samples included in the flow mean; D and I are the eastward declination and downward inclination; K is the dispersion parameter (Fisher, 1953); α_{95} is the angular interval of 95% confidence in the mean direction. (1) See text

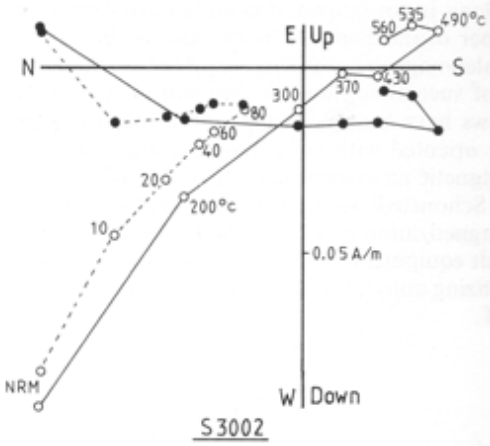

Fig. 4. Comparison of A.F. and thermal demagnetization on two specimens of the core S3002. *Dashed line* for the A.F. demagnetization. *Open and closed circles* used as in Fig. 2

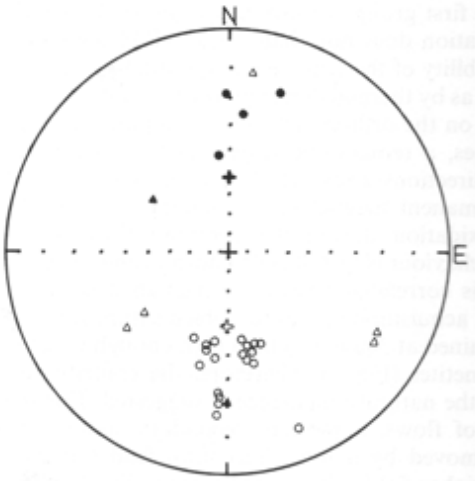

Fig. 5. Stereographic plots of flow-averaged directions. *Solid (open) symbols* indicate downward (upward) directed magnetization vectors. *Triangles* represent the transitional directions rejected from the mean calculation. The *crosses* give the axial dipole direction

Mean paleomagnetic direction and its significance

The stereographic projection of Fig. 5 shows clearly that the 30 directions do not have a Fisherian distribution, making it more difficult to interpret the mean direction and precludes a clear determination of the paleosecular variation. At least two main factors contribute to this situation:

1) Similar paleomagnetic directions of different units may represent repeated sampling of the earth's magnetic field at a particular time, making clusters in the distribution. For example, the most divergent transitional direction ($D=120$, $I=-15$) recorded in two flows S18 and S28, 5 km from one another, has the highest probability of depicting the same event. On the other hand, the reverse directions are distributed principally in three paleomagnetic groups (a: south-east declination, b: south declination and shallow inclination, c: south-west declination) which are found at the different sites. Hence, we propose a time correlation between sites (Fig. 6). The clusters of directions probably indicate a very short time interval between successive flows.

2) The second factor is that some directions are far from the dipole direction and contribute to a large scatter in the distribution. Working with one of the best data sets of more than 2,000 lava flows in Iceland, Kristjansson and McDougall (1982) have shown that it is not easy to separate the transitional from the regular geomagnetic field behaviour to provide the Fisher analysis characteristics of the paleosecular variation. Nevertheless, in recent analyses of worldwide paleosecular variation, a cutoff at colatitude greater than 40 degrees was applied to the VGPS to filter transitional data linked to reversals or excursions (Merrill and McElhinny, 1983; McFadden and McElhinny, 1984). Directions for flow numbers S5, S6, S18, S27, S28, S32 and S33 may be filtered out if we assume they are related to the reversal. The mean direction for all flows after the normal directions have been inverted by 180 degrees is: declination = 177.0; inclination = −32.2; $K=8.9$; $N=30$; $\alpha_{95}=9.3°$; and after the elimination of the seven previous directions: declination = 179.0; inclination = −34.2; $K=27.6$; $N=23$; $\alpha_{95}=5.9°$. Whichever set is selected, we ob-

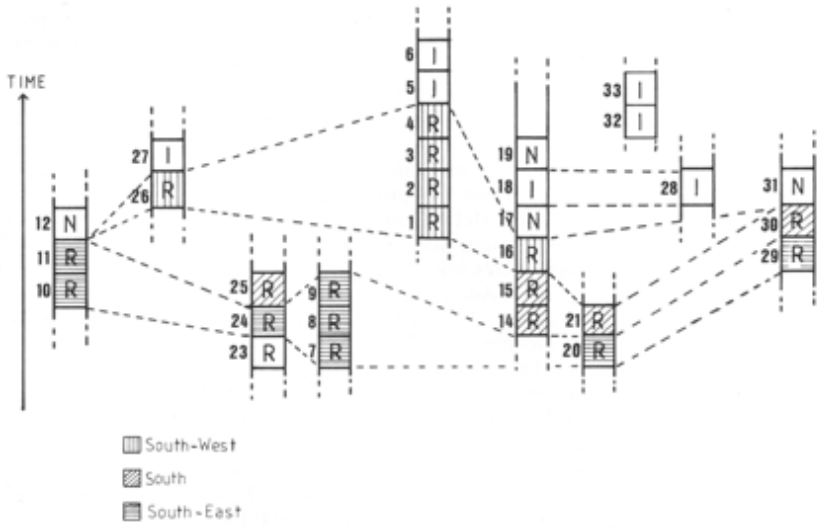

Fig. 6. Attempt at correlation of mean flow directions between sites. Each site shows the stratigraphic position of the flows, and they are diplayed along a north-south trend (see Fig. 1). *R*, *I*, *N* represent, respectively, reverse, intermediate, normal polarities. In the reverse population, three groups have been defined. Only flow No. 23 cannot be correlated with other sites. We are not able to correlate the normal directions, but the diagrams show that they overlay the reverse directions

serve a stability of the mean direction. We consider that a mean direction $D=179$, $I=-34$ is the best estimate of the Miocene mean paleomagnetic field direction in Syria. We think, however, that more data are necessary for a good estimation of the scatter of directions around the mean (i.e. paleosecular variation).

Comparison with data from Africa and Arabia

For the Arabian plate, only very few paleomagnetic studies have been reported and a comparison with the African poles is essential. In order to take into account the opening of the Red Sea, the pole and angle of rotation given by Le Pichon and Francheteau (1978) is used to correct Miocene Arabian data which pre-date the opening.

The selection of reliable African or Arabian data is not easy. The first step for a compilation of data is to ensure that each mean direction corresponds to a good averaging of all the variations of the magnetic field. As nearly all results have been obtained from volcanic rocks, problems arose in the averaging of the paleosecular variation in many cases. A second criterion is the tectonic stability on a regional scale. Some studies which have been undertaken in tectonically active areas, for example the Afar region (Pouchan and Roche, 1971), must be rejected; the results obtained for the Tiberia province in the Lebanon mountains (Nur and Helsley, 1971; Ron et al., 1984) cannot be accepted in a compilation because of the large block rotations which occurred on that side of the Levant fault. The third criterion is a good knowledge of the age of the formations used.

Some compilation of data for Africa has been done recently. In that of Tauxe et al. (1983), the important weight given to the Canary data made it unreliable. The review of Kellog and Reynolds (1983) needs a few modifications. For the Kapiti phonolite (Patel and Gracii, 1972), the semi-angle of confidence ($\alpha_{95}=17°$) is too large to allow its use. The Lybian Garian volcanics have been re-dated as Pliocene (Ade-Hall et al., 1975b). For the Jebel Soda basalts, other data obtained by Ade-Hall et al. (1975a) have been added to those of Schult and Soffel (1973). Finally, we estimate that only six Miocene African poles meet our criteria (Table 2). Nevertheless, the use of the Libyan and Algerian data for the calculation of the mean is questionable. The As-Sarat data (Kellog and Reynolds, 1983) is the unique available data for Arabia.

Table 2. Miocene poles for Africa and Arabia

	VGP		
	Latitude (N)	Longitude (E)	
Turkana lavas	85	163	Reilly et al. (1976)
Rift valley (Kenya)	87	187	Reilly et al. (1976)
Ethiopian lavas	82	200	Musset and Ade-Hall (1975)
Cavallo massif	88	154	Bobier and Robin (1969)
Canary Islands	82	114	Watkins (1973)
Lybia Jebel Soda	73	195	Ade-Hall et al. (1975a)
As Sarat (Arabia)[a]	81	236	Kellog and Reynolds (1983)
Mean ($N=7$)	84	188	$K=138$ $\alpha_{95}=5.2°$
This study	75	220	
This study[a]	76	207	

[a] After rotation of Arabia with the pole and angle of rotation 36.5 N, 18.0 E, 3.25° (Le Pichon and Francheteau, 1978)

The Miocene paleomagnetic pole determined for Arabia and Africa provides an expected paleomagnetic direction for our sampling area of $D=180$, $I=-46$. This calculation takes into account the opening of the Red Sea. A good agreement exists between the observed declination and the expected declination, while there is a discrepancy of 12 degrees between the two inclinations. Shallow inclinations have also been found on Tertiary Egyptian volcanics (Hussain et al., 1979; Schult et al., 1981; Hussain and Aziz, 1983). This problem might be due to an incomplete averaging of the secular variation or to a long-term variation in the dipole field.

Conclusions

The correlations of flows between sites and the single change of polarity from reverse to normal allow us to assess

the short duration of this volcanism. Despite the problem of a non-fisherian distribution, we believe that the mean declination is a good marker and so we conclude that no tectonic rotation has occurred in this area south of Damascus since 20 Ma.

Acknowledgements. We thank G. Carlier and J.F. Parrot for their help during the field work and for helpful comments on the geological context. G. Giannerini and G. Feraud from the University of Nice provided us with the radiometric data. This work was supported by O.R.S.T.O.M.

References

Ade-Hall, J.M., Reynolds, P.H., Dagley, P., Musset, A.E., Hubbard, T.P.: Geophysical studies of North African Cenozoic Volcanic Areas: II. Jebel Soda, Libya. Canadian J. Earth Sci. **12**, 1257–1264, 1975a

Ade-Hall, J.M., Gerstein, S., Gerstein, R.E., Reynolds, P.H., Dagley, P., Musset, A.E., Hubbard, T.P.: Geophysical studies of north African cenozoic volcanic ares.: III. Garian, Libya. Canadian J. Earth Sci. **12**, 1264–1272, 1975b

Bobier, C., Robin, C.: Etude paleomagnetique du massif eruptif de Cavallo (nord-Constantinois, Algerie), C.R. hebd. seanc. acad. sci. **269**, ser D, 134–137, 1969

Bogue, S.W., Coe, R.S.: Back to back paleomagnetic reversal records from Kauai. Nature **295**, 399–401, 1982

Fisher, R.A.: Dispersion on a sphere. Proc. R. Soc. London, Ser. A, **217**, 295–305, 1953

Freund, R.: A model of the structural development of Israel and adjacent areas since upper cretaceous times. Geol. Mag. **102**, 189–205, 1965

Freund, R., Tarling, D.H.: Preliminary mesozoic paleomagnetic results from Israel and inferences for a microplate structure in the Lebanon. Tectonophysics **60**, 189–205, 1979

Gregor, C.B., Mertzman, S., Nairn, A.E.M., Negendank, J.: The paleomagnetism of some mesozoic and cenozoic volcanic rocks from the Lebanon. Tectonophysics **21**, 375–395, 1974

Hussain, G.A., Schult, A., Soffel, H.: Paleomagnetism of the basalts of Wadi Abu Tereifiya, Mandisha and dioritic dykes of Wadi Abu Shihat, Egypt. Geophys. J.R. Astron. Soc. **56**, 55–63, 1979

Hussain, G.A., Aziz, Y.: Paleomagnetism of Mesozoic and Tertiary rocks from East El Owenat area, southwest Egypt. J. Geophys. Res. **88**, 3523–3529, 1983

Kellog, K.S., Reynolds, R.L.: Opening of the Red Sea: constraints from a paleomagnetic study of the As Sarat volcanic field, South western Arabia. Geophys. J.R. Astron. Soc. **74**, 649–665, 1983

Kristjansson, L., McDougall, I.: Some aspects of the late tertiary geomagnetic field in Iceland. Geophys. J.R. Astron. Soc. **68**, 273–294, 1982

Le Pichon, X., Francheteau, J.: A plate tectonic analysis of the Red Sea – Gulf of Aden area. Tectonophysics **46**, 369–406, 1978

McFadden, P.L., McElhinny, M.W.: A physical model for paleosecular variation. Geophys. J.R. Astron. Soc. **78**, 809–830, 1984

Merrill, R.T., McElhinny, M.W.: The earth's magnetic field: Its history, origin and planetary perspective. International geophysics series, vol. 32, 1983

Musset, A.E., Ade-Hall, J.M.: Paleomagnetism and potassium argon dating of Ethiopian cenozoic volcanic areas. Eos. Trans. Am. Geophys. Un. **56**, 902, 1975

Nur, A., Helsley, C.E.: Paleomagnetism of tertiary and recent lavas of Israel. Earth Planet. Sci. Lett **10**, 375–379, 1971

Patel, J.P., Gracii, P.: Paleomagnetic studies of the Kapiti Phonolite of Kenya. Earth Planet. Sci. Lett. **16**, 213–218, 1972

Pouchan, P., Roche, A.: Etude paleomagnétique de formations volcanique du territoire des Afars et des Issas. C.R. hebd. seanc. acad. sci. Paris **272**, ser. D, 531–534, 1971

Prevot, M., Mankinen, E.A., Gromme, C.S., Coe, R.S.: How the geomagnetic field vector reverses polarity. Nature **316**, 230–234, 1985

Reilly, T.A., Raja, P.K.S., Musset, A.E., Brock, A.: The paleomagnetism of late cenozoic volcanic rocks from Kenya and Tanzania. Geophys. J.R. Astron. Soc. **45**, 483–494, 1976

Ron, H., Freund, R., Garfunkel, Z., Nur, A.: Block rotation by strikeslip faulting: Structural and paleomagnetic evidence. J. Geophys. Res. **89**, 6256–6270, 1984

Schult, A., Soffel, H.: Paleomagnetism of tertiary basalts from Libya. Geophys. J.R. Astron. Soc. **32**, 373–380, 1973

Scult, A., Hussain, A.G., Soffel, H.C.: Paleomagnetism of Upper Cretaceous volcanics and Nubian sandstones of Wadi Natash. SE Egypt and implications for the polar wander path for Africa in the Mesozoic. J Geophys. **50**, 16–22, 1981

Tauxe, L., Besse, J., Labrecque, J.: Paleolatitude from DSDP leg 73 sediments cores: Implications for the apparent polar wander path for Africa during the late Mesozoic and Cenozoic. Geophys. J.R. Astron. Soc. **73**, 315–325, 1983

Van Dongen, R.G., Van der Voo, R., Raven, Th.: Paleomagnetic research in the Central Lebanon mountains and in the Tartous area (Syria). Tectonophysics **4**, 35–53, 1967

Watkins, N.D.: Paleomagnetism of the Canary Islands and Madeira. Geophys. J.R. Astron. Soc. **32**, 249–267, 1973

Received October 28, 1985; revised February 3, 1986
Accepted February 20, 1986